Journal of Chromatography A, 1216 (2009) 7388–7393

Contents lists available at ScienceDirect

Journal of Chromatography A

journal homepage: www.elsevier.com/locate/chroma

Synthesis of penetrable macroporous silica spheres for high-performance liquid chromatography

Jun-Xia Wei [a], Zhi-Guo Shi [a,c,*], Fei Chen [a], Yu-Qi Feng [a,c], Qing-Zhong Guo [b]

[a] Department of Chemistry, Wuhan University, Wuhan 430072, China
[b] School of Materials Science and Engineering, Wuhan Institute of Technology, Wuhan 430073, China
[c] Key Laboratory of Analytical Chemistry for Biology and Medicine (Wuhan University), Ministry of Education, Wuhan 430072, China

ARTICLE INFO

Article history:
Available online 3 May 2009

Keywords:
Silica
Microspheres
Liquid chromatography
Fast separation
Low backpressure

ABSTRACT

Silica microspheres have been synthesized by phase separation and sol–gel transition coupled with emulsion method. The as-obtained material is characterized by scanning electron microscopy, nitrogen sorption, elemental analysis and particle size distribution measurements. The results demonstrated that the material featured with hierarchically porous structure, possessing both mesopores and penetrable macropores. The mesopores provide large surface area while the macropores traverse the silica particles, which may facilitate fast mass transfer as well as guarantee low backpressure when such materials are used for packed high-performance liquid chromatography (HPLC) column. Therefore, their preliminary applications as HPLC packings in fast separation and low-pressure separation have been attempted in the present study. Benzene, benzaldehyde and benzyl alcohol were separated within two minutes on the silica column at a flow rate of 7 mL min^{-1}. Vitamin E mixtures can also be baseline separated at a high flow rate of 8 mL min^{-1}. In addition, thirteen aromatic hydrocarbons were well separated on the octadecyl-bonded silica (ODS) column. In comparison with a commercial Kromasil ODS column, the pressure of the proposed column is much lower (<1/2) under the same chromatographic conditions, while comparable separation efficiency can be achieved.

1. Introduction

High-performance liquid chromatography (HPLC) is widely used in modern industry, from factory quality control to massive manufacture of high value added products, especially for complex systems such as biological samples, natural products, drugs, etc. [1].

One of the kernel parts of HPLC is its column packing, which significantly determines the performance of a HPLC system. To satisfy more and more complicated application requirements, much effort has been devoted to the fabrication of column packings with various compositions and different porous structures, from polymer to inorganic oxides (silica, zirconia and titania), from microporous to mesoporous and macroporous structure, etc. [2]. Among these, silica is the most appreciated packing for its high mechanical strength, temperature and solvent resistance, facile surface functionalization, availability as well as benign biocompatability. It overwhelms about 80% market share in chromatographic packings. As the pore size, volume, connectivity, depth, particle size, size distribution and morphology are vital for the behavior of silica packings, designing silicas with various morphologies and porous structures to fully exploit their potential has raised intensive interest for several decades [3–5].

To some extent, decreasing particle size, lowering pore depth or increasing pore size may improve the separation performance of a silica material. However, many problems such as high backpressure, small surface area or low mechanical strength associated with the above properties may arise. To balance the performance and operational convenience, porous silicas with particle sizes ranging from 3 to 10 μm are currently most widely used in typical HPLC separations.

In some circumstances, the whole performance of HPLC is not always a criteria, and attention can be laid on respective aspects such as separation speed, column pressure, capacity, etc. Non-porous silicas [6–8], sub-micrometer-sized silicas [9–13], solid-core-porous-surface silicas [14,15] and monolithic silicas [16–18] have been fabricated for specific applications. For instance, non-porous silicas can realize fast separation because of its prompt mass transfer property; sub-micrometer-sized silicas can achieve excellent separation performance for complex samples; monolithic silicas can provide low backpressure as well as fast separation performance. However, these materials have more or less shortcomings in the application or synthesis. Non-porous silicas only afford limited column capacity. High column pressure is always

* Corresponding author at: Department of Chemistry, Wuhan University, Wuhan 430072, China. Fax: +86 27 68754067.
E-mail address: shizg@whu.edu.cn (Z.-G. Shi).

0021-9673/$ – see front matter © 2009 Elsevier B.V. All rights reserved.
doi:10.1016/j.chroma.2009.04.066

a problem in the case of sub-micrometer-sized silicas as column packing. Preparation of monolithic materials is tedious. Especially for large dimension monoliths, shrinkage and crack cannot be easily overcome.

Herein, we reported the synthesis of new silica microspheres featuring with interlacing skeletons and macropores. The skeletons possess numerous mesopores which guarantee high surface area of the material; the macropores, which traverse the microspheres, may realize convective mass transfer. Considering the high porosity of the material, it is expected to overcome shortcomings associated with the above-mentioned materials. Hence, its preliminary application was attempted in low-pressure and fast HPLC separation.

2. Experimental

2.1. Chemicals and materials

Tetraethoxylsilane (TEOS) and octadecyl trimethoxysilane were obtained from the Chemical Factory of Wuhan University (Wuhan, China). Polyethylene oxide (PEO, molecular weight: 100,000), paraffin oil, ethanol, toluene, and hydrochloric acid were purchased from Shanghai General Chemical Reagent Factory (Shanghai, China). Aromatic hydrocarbon standard mixtures and vitamin E standards (α-, β-, γ- and δ-) were purchased from Sigma Aldrich (St. Louis, MO, USA). HPLC-grade methanol was obtained from Fisher (Loughborough, UK). Ultrapure water was produced on a Nanopure (Barnstead, Dubuque, IA, USA) water purification system.

2.2. Synthesis of the silica microspheres

90 mL TEOS, 150 mL hydrochloric acid (0.01 mol L^{-1}) and 15.0 g PEO were mixed at 333 K for 2 h to get a transparent solution. Then it was added into a 2-L three-neck round-bottom flask containing 800 mL paraffin oil. The whole solution was vigorously stirred for 10 min before it was incubated in a water bath at 323 K. The stirring was kept at 2000 rounds per minute. Twenty hours later, white precipitate appeared. The product thus obtained was flushed with massive petroleum ether and ethanol consecutively. Thereafter, it was hydrothermal treated at 473 K for 10 h and calcinated at 873 K for 2 h. Finally, the silica microspheres were acquired.

Since a wide distribution of particles may be detrimental to the application performance in HPLC, prior to use, the microspheres were subject to size-classification by liquid elutriation. Spheres with size ranging from 4 to 6 μm were collected for further usage. The yield was found to be 62% of the total product.

2.3. Surface grafting of octadecyl moieties onto the silica spheres

Surface modification was carried out as follows: 10 g of silica spheres was activated in 6 mol L^{-1} of hydrochloric acid for 24 h, which were then washed to neutral pH and fully dried at 433 K for at least 5 h. Thereafter, 5 g of octadecyl trimethoxysilane, 200 mL of anhydrous toluene and silica were mixed and refluxed under nitrogen atmosphere. Twenty hours later, octadecyl-bonded silica (ODS) thus obtained was washed with toluene, ethanol and water in sequence. Finally, it was dried for further usage.

2.4. Characterization of the silica spheres and the ODS

A scanning electron microscope of JSM-35CF (JEOL, Tokyo, Japan) was used to study the morphologies of the silica spheres. A Malvern Mastersizer 2000 (Worcestershire, UK) instrument was used to investigate the particle size distributions of the materials. A mercury intrusion porosimeter of Autopore IV 9500 (Micromeritics, Atlanta, GA, USA) and a nitrogen porosimeter of SA 3100 Plus (Beckman Coulter, Miami, FL, USA) were employed to measure their macroporous and mesoporous structures, respectively. Prior to analysis, the sample was outgassed at 393 K for 10 h. The specific surface area value was calculated according to the BET (Brunauer–Emmett–Teller) method at P/P_0 between 0.05 and 0.2. The mesopore parameters were evaluated from the adsorption branch of the isotherm based on BJH (Barrett–Joyner–Halenda) model. A PerkinElmer (Shelton, CT, USA) 2400 element analyzer was adopted to determine the carbon content of the ODS.

2.5. Apparatus and chromatographic applications

Column packing was achieved on an air driven liquid pump from Haskel (Burbank, CA, USA). The above-prepared silica and ODS were slurry-packed into stainless steel columns (15 cm × 4.6 mm I.D.) at 6000 psi for 20 min, respectively. Then the columns were closed with endfittings and were ready for HPLC applications.

The chromatographic system consisted of a Rheodyne (Cotati, CA, USA) 7725i injector equipped with a 20-μL sample loop, a Waters 1525 binary pump and a Waters 2487 UV–vis spectrophotometric detector. Data were collected and processed by Empower version 5.0 (Waters, Milford, MA, USA) data analysis software. A Kromasil ODS column (150 mm × 4.6 mm I.D.) from Akzo-Nobel (Amsterdam, Netherlands) was used for comparison. Separations were carried out at a column temperature of 298 K. All the separations were performed in triplicate.

3. Results and discussion

3.1. Characterization of the silica microspheres

Fig. 1 shows the scanning electron microscopy (SEM) image of the silica microspheres. Apparently, the spheres were composed of skeletons and observable macropores, which were interwoven with each other, forming a net structure. From the bar gauge of the image, it can be calculated that the skeleton size was around 0.8 μm while the macropore size was in the range of 0.6–1.3 μm. Though macropores can be easily observed from the surface, to further investigate whether the macropores are penetrable or evenly distributed within the silicas, the spheres were used as sacrificing templates for producing carbon replicas [19]. Fig. 2 demonstrates the SEM images of a penetrable silica ((a) and (b)) and its carbon replica ((c) and (d)). It can be found that the carbon replica resembles its template, with spherical shape and noticeable macropores on the surface. The result fully revealed the internal structure of the silica. Only when the macropores are penetrable and interconnected within the silica sphere, a spherical carbon can be obtained. Therefore, we can deduce that the macropores exist not only on

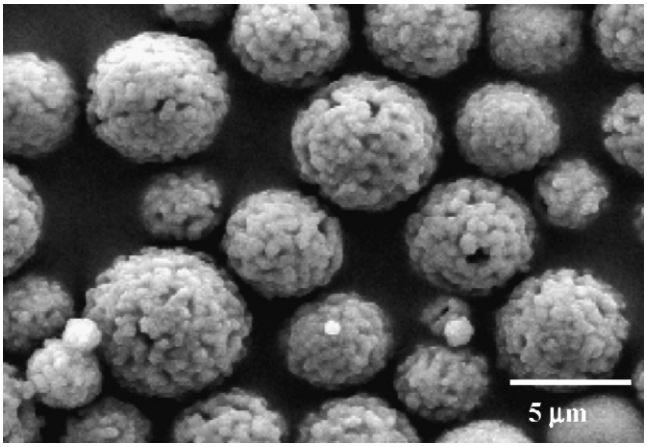

Fig. 1. Scanning electron micrograph of the silica microspheres.

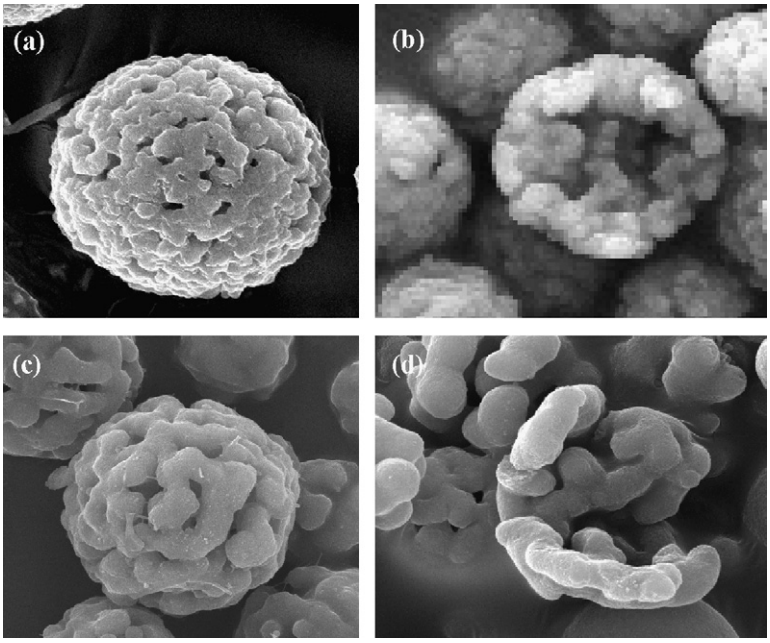

Fig. 2. Scanning electron micrographs of the penetrable spheres: (a and b) silica, (c and d) carbon.

the silica's surface but also within the interior. The fractured SEM images of Fig. 2(b) and (d) also testified this deduction.

Fig. 3 displays the nitrogen sorption isotherm and pore size distribution curve (PSD curve, Inset) of the silica material. A typical isotherm for mesoporous material suggested the presence of a large quantity of mesopores in the material. From the inset PSD curve, it can be found that the mesopores mainly centered at 21 nm. No significant adsorption uptake at pressures below $0.05P_o$ indicates micropores were absent or very limited within the silica microspheres. The BET specific surface area and total mesopore volume were calculated to be 287 $m^2\ g^{-1}$ and 1.1 $cm^3\ g^{-1}$, respectively.

3.2. Mechanism for the porous structure formation of the silica microspheres

The formation of interwoven skeletons and macropores of the silica microspheres was ascribed to synergetic interaction of phase separation and sol–gel transition (or gelation) in confined emulsion droplets. It has been documented that, in the presence of PEO, a sol–gel transition process is generally accompanied by a phase separation [20,21]. The relative speeds of gelation and phase separation, which determine the structure of the final material, are highly related to synthesis parameters such as reactant ratio, solvent, temperature, etc. Therefore, it is possible to realize structural control of the material by deliberate selection of proper synthesis conditions. Under some circumstances, when the gelation and phase separation progress in a balanced manner, materials with interlacing phases of skeletons and solvents can be formed. After necessary treatments such as drying and calcination, the solvent phase evolves into macropores. As a result, the as-prepared silica microspheres demonstrated macroporous structure. In addition to macropores, mesopores also exist on the skeletons of the material. Their formation may be ascribed to the post-hydrothermal treatment, which has been reported by several publications [20,21].

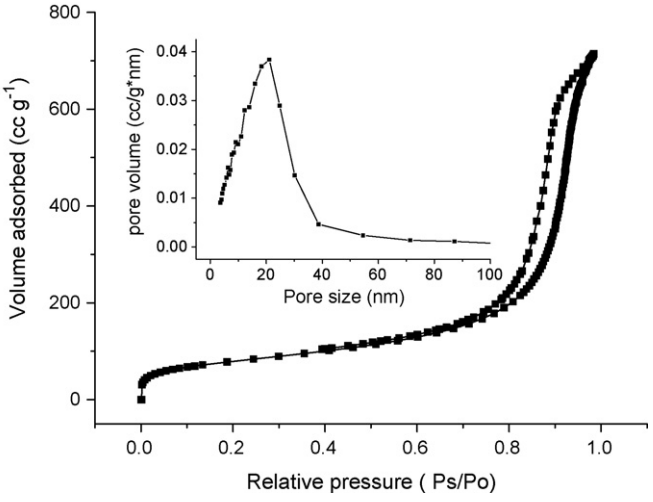

Fig. 3. Nitrogen adsorption–desorption isotherms and the mesopore size distribution (inset) for the silica microspheres.

3.3. Mechanical strength of the silica microspheres

Generally highly porous materials suffer from low mechanical strength, which severely limits their applications. To fully understand the mechanical characteristic of the newly prepared silica, its structural strength was investigated. Figs. 4 and 5 show the particle size distribution curves and the SEM images of the penetrable silica before (a) and after (b) being packed into a HPLC column at 6000 psi for 20 min. It can be found that the packing pressure has little influence on the size distributions as well as the integrity of the particles. Apparently, the silica particles have satisfactory mechanical strength.

3.4. HPLC applications

As the silica microspheres feature with penetrable macropores and high porosity, it may be useful in fast separation or low-pressure separation area. Therefore, their applications in these two aspects have been attempted.

3.4.1. Low-pressure separation

The silica microspheres were covalently bonded with octadecyl functional groups. Elemental analysis revealed that, after modifi-

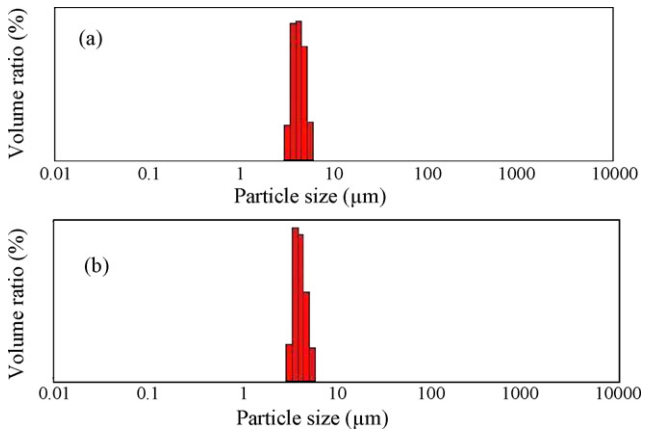

Fig. 4. The particle size distributions of the penetrable silica before (a) and after (b) packing.

cation, the carbon content was 15.1% (w/w). The surface coverage of ODS was calculated to be about 2.4 μmol/m^2. The as-prepared ODS was slurry-packed into a column to evaluate the effectiveness for the separation of aromatic hydrocarbons. For comparison, a Kromasil ODS column, which had the same dimension as the laboratory-prepared ODS column, was also used for the separation of these analytes.

Fig. 6a and b shows the separation of thirteen aromatic hydrocarbons on the Kromasil ODS column and the laboratory-prepared ODS column, respectively. Obviously, the retention of analytes on the Kromasil ODS column was a little stronger than that on the laboratory-prepared ODS column. It may be ascribed to the phase ratio as well as the carbon content of the two columns. Because of the high porosity of the penetrable silica, the laboratory-prepared ODS column contains relative less stationary phase than that of the Kromasil ODS column. The phase ratios calculated for them were 8.26 (laboratory-prepared column) and 3.95 (commercial column), respectively. Obviously, the phase ratio for the laboratory-prepared column is far larger than that of the Kromasil one. Moreover, the carbon content of the laboratory-prepared ODS is a little lower than that of the Kromasil ODS (18.2%, w/w). Therefore, analytes were eluted much faster on the laboratory-prepared column than on the commercial column. Nevertheless, all of the analytes have been baseline separated on both columns. The column efficiencies and the resolutions for two representative analytes (marked as S-1 and S-2 in Fig. 6) of the thirteen were calculated. It was found that on the laboratory-prepared column, the column efficiencies for S-1 and S-2 were 32,000 and 45,000 plates/m, respectively. The resolution for them was 13.47. On the Kromasil column, the column efficiencies for S-1 and S-2 were 27,000 and 37,000 plates/m, respectively. The

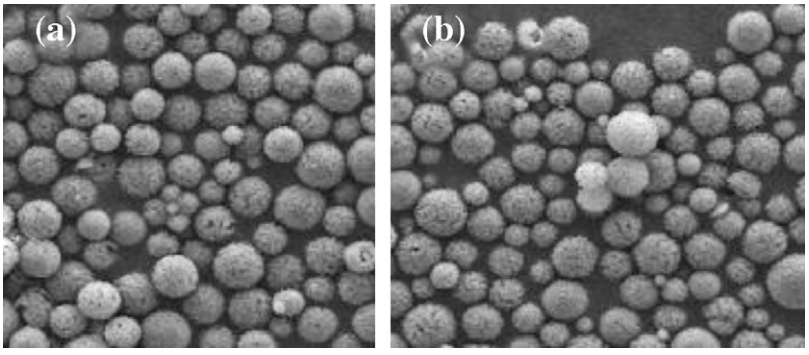

Fig. 5. The SEM micrographs of the penetrable silica particles before (a) and after (b) packing.

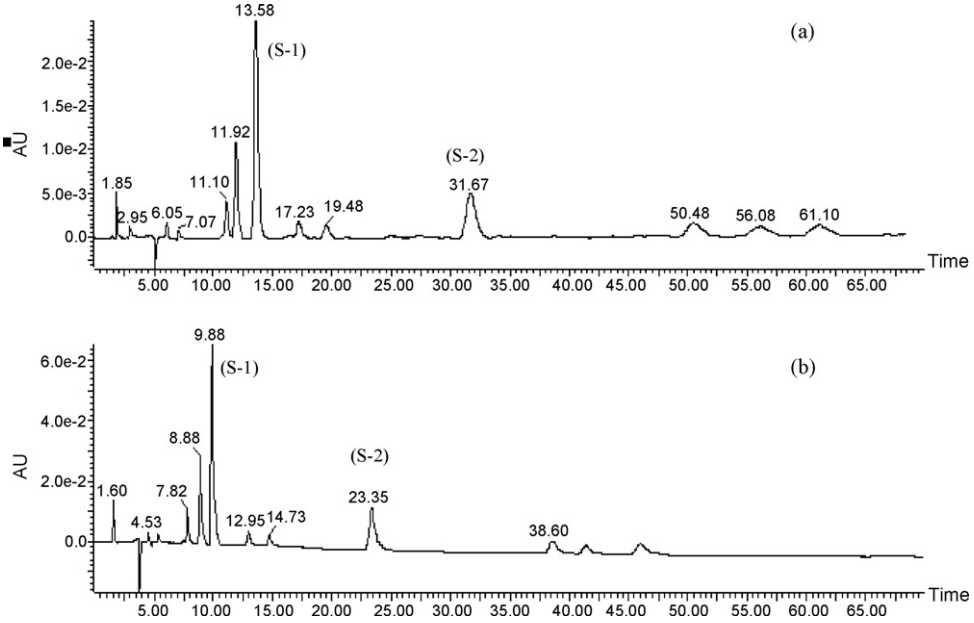

Fig. 6. Separation of aromatic hydrocarbons on (a) a Kromasil ODS column (15 cm × 4.6 mm I.D.) and (b) the laboratory-prepared penetrable ODS column (15 cm × 4.6 mm I.D.); mobile phase: 80% methanol–water (v/v); flow rate: 1 mL min^{-1}. Analytes: Aromatic hydrocarbon mixtures.

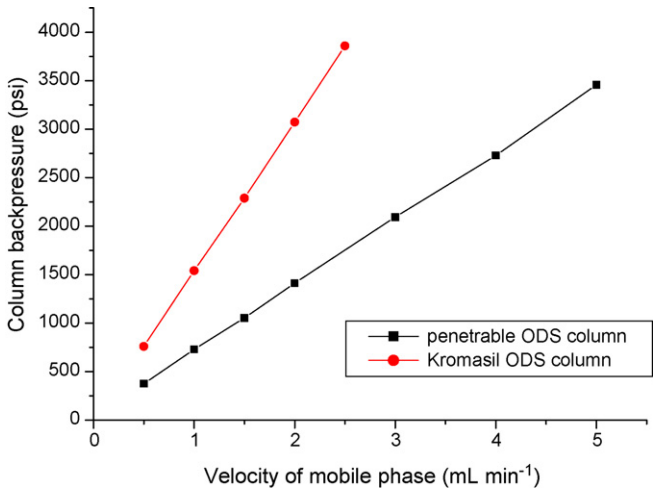

Fig. 7. Comparison of the backpressure/flow behaviors of the penetrable ODS column (15 cm × 4.6 mm I.D.) and the commercial Kromasil ODS column (15 cm × 4.6 mm I.D.); mobile phase: 80% methanol–water (v/v).

resolution for them was 12.06. Obviously, the results demonstrate that the efficiencies are comparable on these two columns.

The backpressure/flow behaviors on the penetrable ODS column and the Kromasil ODS column are compared in Fig. 7. It is found that the corresponding pressure on the laboratory-prepared ODS column was about half of that of the Kromasil ODS column at the same velocity (1–3 mL min^{-1}). As the flow rate was raised to above 4 mL min^{-1}, the pressure on the Kromasil ODS column was too high, exceeding the pressure limit of the instrument. Fig. 8 demonstrates the particle size distributions of the penetrable silica (a) and the Kromasil packing (b). It can be found that both of the packings have similar particle size distributions, with a mean size concentrated at ca. 5 μm. Since their particle sizes are quite similar, the backpressure difference should be originated from the different porous structures. Probably, the penetrable macropores in the laboratory-prepared ODS would facilitate mobile phase to flow through the particles. Therefore, low backpressure can be realized on this column. The permeabilities of the laboratory-prepared ODS column and the Kromasil ODS one were calculated to be 9.6×10^{-10} and 4.5×10^{-10} cm^2, respectively. Apparently, the laboratory-prepared ODS column is suitable for low backpressure separations.

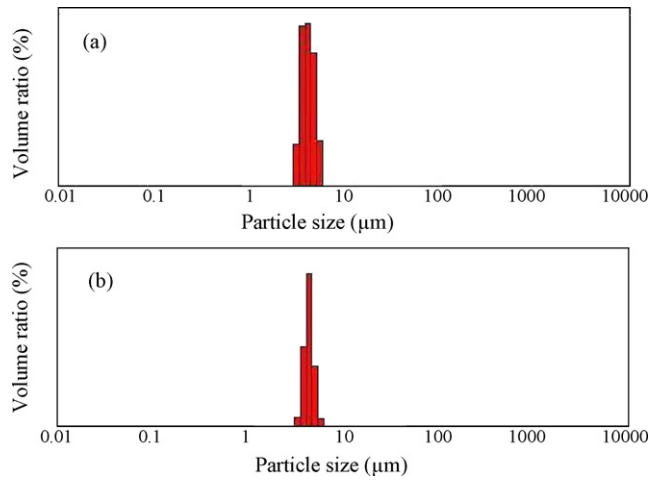

Fig. 8. The particle size distributions of the penetrable silica (a) and the Kromasil packing (b).

3.4.2. Fast separation

In many circumstances such as massive product quality inspection and preparative chromatography, fast separation is admirable because it can increase the work efficiency. However, it is difficult to realize fast separation on traditional packings. As the flow rate of mobile phase increases, the column pressure increases sharply. Meanwhile, the column efficiency decreases dramatically because of the slow mass transfer on these packings. However, the as-prepared silica microspheres are characterized by penetrable macropores, which may decrease the flow resistance of mobile phases and facilitate mass transfer of analytes on this packing. In such a case, the new material would be promising for fast separation applications.

Fig. 9 demonstrates the separation of benzene, benzaldehyde and benzyl alcohol with mobile phase of hexane/isopropyl alcohol (100/1, v/v) at different velocities of 1–7 mL min^{-1}. Obviously, as the velocity of the mobile phase increased, fast separation was realized. At a velocity of 7 mL min^{-1}, the analytes can be baseline separated within 2 min and the column backpressure was only 2447 psi. In addition to benzene derivatives, separation of vitamin E mixture was also tested on this column. As shown in Fig. 10, even when the flow rate of the mobile phase reached 8 mL min^{-1}, the analytes can also be baseline separated, which would be very helpful for the massive purification of such analytes. However, it can also be found that as the velocity increased, the column efficiency decreased gradually.

Fig. 11 displays the van Deemter plots for the penetrable ODS column with naphthalene, biphenyl and phenanthrene as analytes. It revealed that as the velocity of mobile phase increased from 0.5–3 mL min^{-1}, the plate height almost kept constant; however, when the velocity further increased up to 4–5 mL min^{-1}, the plate

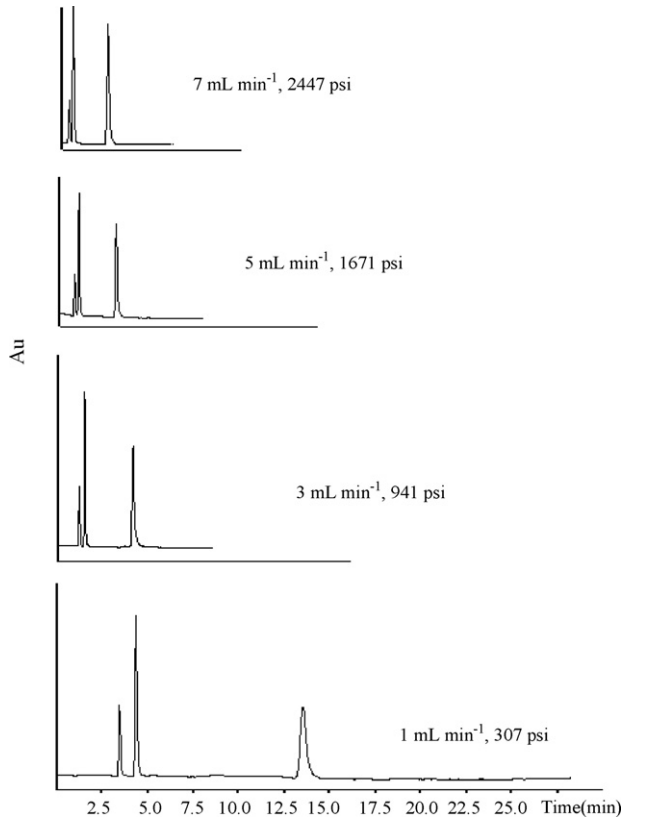

Fig. 9. Separation of benzene derivatives with mobile phases at different flow rates on penetrable silica column (15 cm × 4.6 mm I.D.); mobile phase: hexane/isopropyl alcohol (100/1, v/v). Analytes: Benzene, benzaldehyde and benzyl alcohol (from the left to the right).

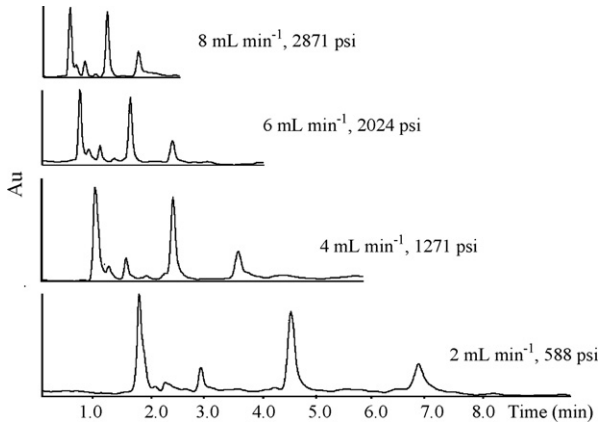

Fig. 10. Separation of vitamin E mixture with mobile phases at different flow rates on penetrable silica column (15 cm × 4.6 mm I.D.); mobile phase: (hexane/isopropyl alcohol = 100/0.6, v/v); Samples: α-, β-, γ- and δ-vitamin E (from the left to the right).

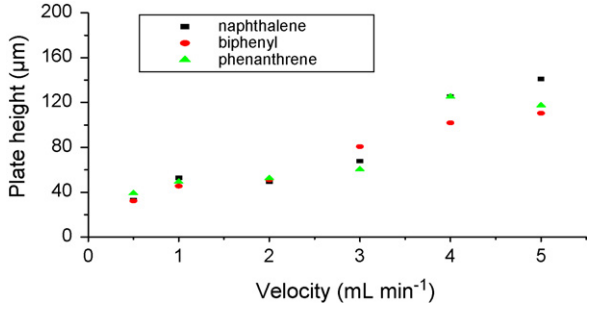

Fig. 11. van Deemter plots for the penetrable ODS column (15 cm × 4.6 mm I.D.) with naphthalene, biphenyl and phenanthrene as solutes; mobile phase: 80% methanol–water (v/v).

height increased obviously, indicating a notable column efficiency decrease in this velocity range. Probably, the sizes of the silica skeletons, the macropores and the interstitial voids between the particles account for this phenomenon. If these parameters can be designed to match with each other, the column efficiency would be further improved. Nevertheless, to some extent, the new packing can realize fast separation.

3.5. Stability

Column stability was investigated with benzene derivatives using a mobile phase consisting of hexane/isopropyl alcohol (100/1, v/v). No loss in the model analytes resolution was observed after the column was operated with high flow rate (7 mL min^{-1}) for 3 month and the backpressure of the column kept constant (<3% around 2450 psi). Mechanical strength studies indicate that the silica spheres are stable to pressures greater than 6000 psi without compression.

4. Conclusions

To conclude, here we proposed a facile way for the synthesis of a silica packing with interlacing skeletons and macropores. Due to the penetrable macroporous structure, large surface area as well as high porosity, the novel material is promising in HPLC applications in terms of low-pressure separation and/or fast separation. Although the column efficiency still needs to be improved, its application in these two aspects has been proved to be successful. The new silica packing, as a useful complementarity to the existing packing materials, is anticipated to contribute to the development of related chromatographic applications.

Acknowledgments

The support of National Nature Science Foundation of China (NSFC 20605015), the National Science Fund for Distinguished Young Scholars (No. 20625516) and the Nature Science Fund of Hubei Province (No. 2005ABA033) are gratefully acknowledged.

References

[1] K.K. Unger, G. Jilge, R. Janzen, H. Giesche, J.N. Kinkel, Chromatographia 22 (1986) 379.
[2] Q.H. Zhang, Y.Q. Feng, S.L. Da, Anal. Sci. 15 (1999) 767.
[3] A. Lind, C. Hohenesche, J.H. Smatt, M. Linden, K.K. Unger, Micropor. Mesopor. Mater. 66 (2003) 219.
[4] J.J. Kirkland, T.J. Langlois, J.J. DeStefano, Am. Lab. 39 (2007) 18.
[5] K. Nakanishi, N. Soga, J. Non-Cryst. Solids 139 (1992) 14.
[6] J.T. Parrish, Nature 207 (1965) 402.
[7] M.Q. Zhang, G.K. Ostrander, Z.E. Rassi, J. Chromatogr. A 887 (2000) 287.
[8] C. Oh, J.H. Lee, Y.G. Lee, Y.H. Lee, J.W. Kim, H.H. Kang, S.G. Oh, Colloid Surf. B-Biointerfaces 53 (2006) 225.
[9] S. Luedtke, T. Adam, K.K. Unger, J. Chromatogr. A 786 (1997) 229.
[10] S. Luedtke, T. Adam, N. Doehren, K.K. Unger, J. Chromatogr. A 887 (2000) 339.
[11] Y.F. Shen, R.D. Smith, K.K. Unger, D. Kumar, D. Lubda, Anal. Chem. 77 (2005) 6692.
[12] M.U. Martines, E. Yeong, M. Persin, A. Larbot, W.F. Voorhout, C.K.U. kubel, P. Kooyman, E. Prouzet, C. R. Chim. 8 (2005) 627.
[13] M. Grun, K.K. Unger, A. Matsumoto, K. Tsutsumi, Micropor. Mesopor. Mater. 27 (1999) 207.
[14] J.J. Kirkland, F.A. Truszkowski, C.H. Dilks Jr., G.S. Engel, J. Chromatogr. A 890 (2000) 3.
[15] J.J. Kirkland, F.A. Truszkowski, R.D. Ricker, J. Chromatogr. A 965 (2002) 25.
[16] D. Lubda, K. Cabrera, K. Nakanishi, H. Minakuchi, J. Sol–Gel Sci. Technol. 23 (2002) 185.
[17] C.D. Liang, S. Dai, G. Guiochon, Chem. Commun. 22 (2002) 2680.
[18] H. Kobayashi, T. Ikegami, H. Kimura, T. Hara, D. Tokuda, N. Tanaka, Anal. Sci. 22 (2006) 491.
[19] R. Ryoo, S.H. Joo, M. Kruk, M. Jaroniec, Adv. Mater. 13 (2001) 677.
[20] K. Nakanishi, N. Soga, J. Non-Cryst. Solids 139 (1992) 1.
[21] Z.G. Shi, Y.Q. Feng, Micropor. Mesopor. Mater. 116 (2008) 701.